

UAV-TRACK VLA: EMBODIED AERIAL TRACKING VIA VISION-LANGUAGE-ACTION MODELS

Qiyao Zhang^{1,7*} Shuhua Zheng¹ Jianli Sun^{2,7} Chengxiang Li^{3,7} Xianke Wu^{4,7}
 Zihan Song^{5,7} Zhiyong Cui⁶ Yisheng Lv² Yonglin Tian^{2,7†}

¹Beijing Institute of Technology, Beijing, China

²Institute of Automation, Chinese Academy of Sciences, Beijing, China

³University of Sanya, Sanya, Hainan, China

⁴Beijing University of Posts and Telecommunications, Beijing, China

⁵Hunan University, Changsha, Hunan, China

⁶Beihang University, Beijing, China

⁷Flying Intelligence Team (Virtual Research Community) [url]

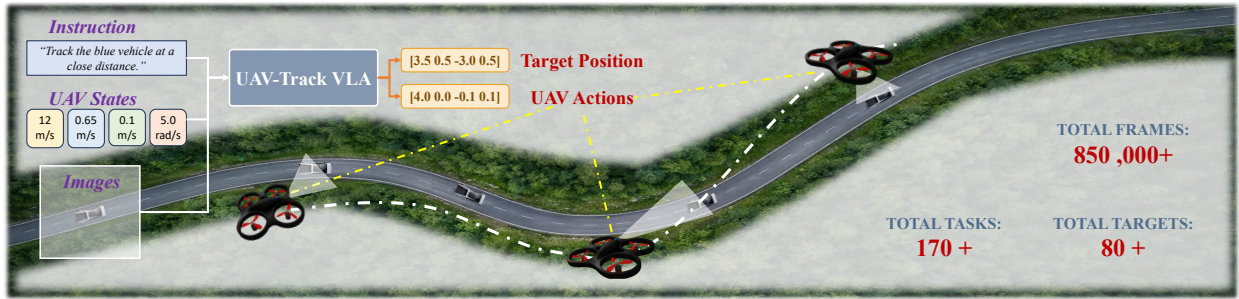


Figure 1: The UAV-Track VLA model follows human instructions to simultaneously predict the target position and continuous UAV flight actions.

ABSTRACT

Embodied visual tracking is crucial for Unmanned Aerial Vehicles (UAVs) executing complex real-world tasks. In dynamic urban scenarios with complex semantic requirements, Vision-Language-Action (VLA) models show great promise due to their cross-modal fusion and continuous action generation capabilities. To benchmark multimodal tracking in such environments, we construct a dedicated evaluation benchmark and a large-scale dataset encompassing over 890K frames, 176 tasks, and 85 diverse objects. Furthermore, to address temporal feature redundancy and the lack of spatial geometric priors in existing VLA models, we propose an improved VLA tracking model, UAV-Track VLA. Built upon the $\pi_{0.5}$ architecture, our model introduces a temporal compression net to efficiently capture inter-frame dynamics. Additionally, a parallel dual-branch decoder comprising a spatial-aware auxiliary grounding head and a flow matching action expert is designed to decouple cross-modal features and generate fine-grained continuous actions. Systematic experiments in the CARLA simulator validate the superior end-to-end performance of our method. Notably, in challenging long-distance pedestrian tracking tasks, UAV-Track VLA achieves a 61.76% success rate and 269.65 average tracking frames, significantly outperforming existing baselines. Furthermore, it demonstrates robust zero-shot generalization in unseen environments and reduces single-step inference latency by 33.4% (to 0.0571s) compared to the original $\pi_{0.5}$, enabling highly efficient, real-time UAV

*The work was done during the internship at Institute of Automation, Chinese Academy of Sciences (3220241221bit.edu.cn).

†Corresponding author (yonglin.tian@ia.ac.cn).

control. Data samples and demonstration videos are available at: https://github.com/Hub-Tian/UAV-Track_VLA.

Keywords Unmanned Aerial Vehicle · Vision-Language-Action Models · Embodied Visual Tracking

1 Introduction

Unmanned Aerial Vehicles (UAVs) are being increasingly utilized to execute complex tasks in real-world environments [1, 2]. As a core perceptual capability, visual tracking serves as the foundation for advanced applications such as inspection, search and rescue, and traffic monitoring[3]. However, contemporary UAV visual tracking predominantly relies on manual flight control, deploying deep learning models on the backend merely for passive target detection or segmentation on transmitted images [4, 5, 6]. This decoupled paradigm fails to achieve autonomous pursuit and dynamic tracking, severely constraining the large-scale deployment and execution efficiency of UAVs in complex scenarios.

Driven by advancements in artificial intelligence, recent years have witnessed a surge in research on Visual Active Tracking (VAT) for UAVs [7, 8, 9]. These approaches empower UAVs to autonomously make decisions and adjust flight postures based on visual feedback, thereby alleviating the reliance on manual control during tracking missions. Nevertheless, the vast majority of existing VAT frameworks are confined to a direct mapping between visual inputs and motor actions, completely omitting the language modality. This critical lack of high-level semantic understanding renders UAVs incapable of executing complex instructions specified by natural language, which in turn limits their applicability in real-world interactive scenarios.

With the rapid evolution of Large Language Models (LLMs) and multimodal fusion technologies, Vision-Language-Action (VLA) models have demonstrated remarkable capabilities in robotic manipulation, autonomous driving, and path planning [10, 11, 12, 13, 14]. In the realm of object tracking, researchers have recently introduced the concept of Embodied Visual Tracking (EVT), formally integrating the language modality into active visual tracking. For instance, pioneering works like TrackVLA[15] have successfully incorporated VLA models into EVT tasks. However, current EVT research predominantly relies on ground-based platforms, such as quadrupedal or wheeled robots. Compared to ground robots constrained to a 2D plane, UAVs possess superior maneuverability in 3D space, offering a much freer tracking perspective. Despite this potential, there remains a glaring absence of dedicated EVT benchmarks and tailored methodologies for UAVs.

Urban outdoor scenarios are characterized by large spatial scales and pronounced target dynamics. Objects such as vehicles and pedestrians exhibit highly heterogeneous motion patterns, which imposes high requirements on the joint extraction of spatial and temporal information for continuous target tracking. Existing UAV active tracking datasets (such as those used in VLA-AN[16]) fail to include targets with complex kinematic behaviors like vehicles, making them ill-suited for the demands of urban traffic scenarios. To train a versatile model capable of robust tracking across diverse targets, it is imperative to construct an EVT dataset that encompasses precise linguistic instructions, heterogeneous tracking objects, and supports continuous UAV motion control.

Furthermore, existing VLA models suffer from significant limitations in dynamic tracking tasks: they not only lack the capacity to process continuous temporal image sequences due to an over-reliance on single-frame spatial feature fusion, but also exhibit poor feature extraction capabilities for high-speed and irregularly moving objects. Consequently, these models struggle to align high-level semantics with low-level continuous flight control, making architectural improvements urgently needed.

To bridge these gaps, we propose a novel embodied UAV tracking benchmark, dubbed UAV-Track, tailored for complex urban scenarios, and introduce structural enhancements to existing VLA models to rectify their shortcomings in temporal feature extraction and cross-modal control alignment. The main contributions of this paper are summarized as follows:

- We construct the first vision-language dataset for embodied UAV tracking in urban environments. Collected within the CARLA simulator, this dataset comprises over 890,000 frames, fine-grained spatial instructions, and diverse tracking targets including vehicles and pedestrians, thereby filling the void in semantic-level EVT benchmarks for UAVs.
- We propose a novel uav tracking vla method with temporal enhancement and spatial guidance. This model incorporates a temporal compression network to extract historical motion evolution patterns. Concurrently, it employs a parallel dual-branch decoding architecture: a spatial-aware auxiliary grounding head injects geometric priors, while a flow matching action expert generates a 25-step continuous displacement sequence, effectively aligning visual semantics with UAV kinematic control.

- We conduct comprehensive experimental evaluations in CARLA. The results demonstrate our model’s superior performance in cross-modal alignment, continuous tracking capability, and robust zero-shot generalization across varying environments, target speeds, and spatial instructions.

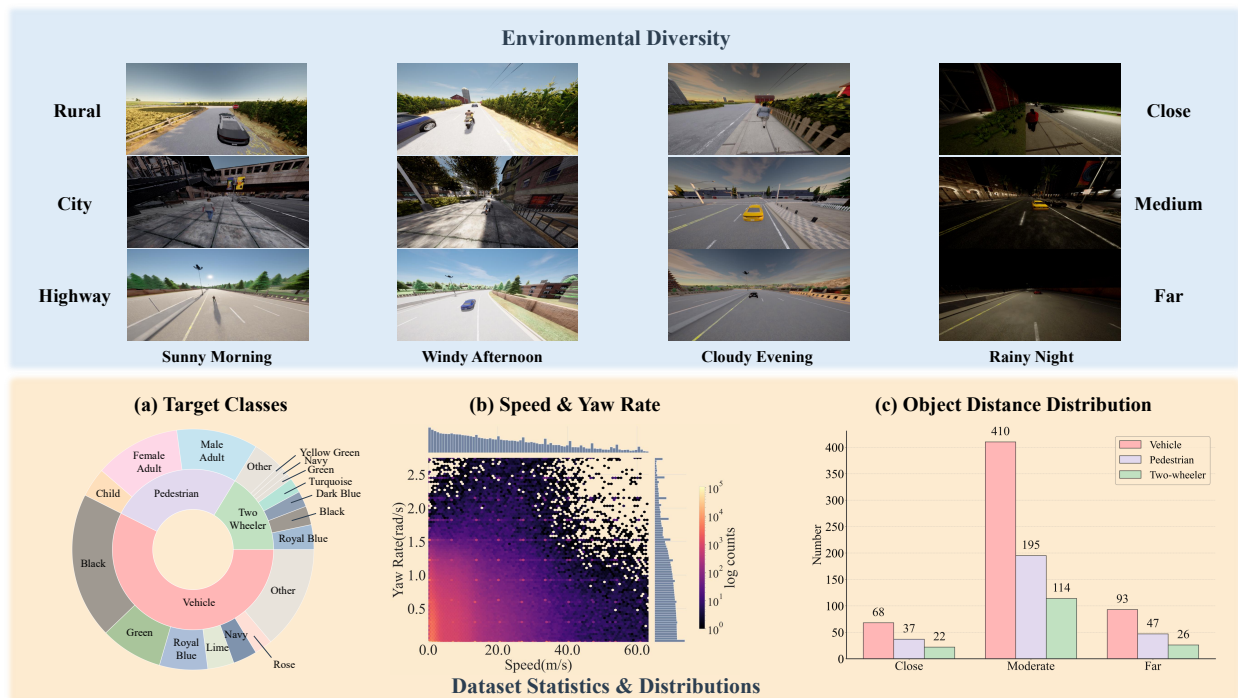


Figure 2: A comprehensive overview of the multidimensional diversity of our benchmark dataset. Top: Visualization of environment diversity. Middle: Task paradigms and overall dataset scale of the UAV-Track benchmark. Bottom: Quantitative distribution of target categories, kinematic parameters, and tracking distances.

2 Related Work

2.1 Embodied Visual Tracking

As a crucial branch of computer vision, UAV Visual Tracking has advanced significantly to address aerial visual characteristics and hardware constraints [4, 6, 5]. Recent research has shifted from merely improving tracking robustness [17, 4, 6] to optimizing model efficiency and semantic alignment [18, 5, 19, 20]. For instance, Aba-ViTrack [5] reduces computational overhead via background aware token computation, while AVTrack-MD [18] employs multi-teacher knowledge distillation for efficient representation. Similarly, SGLATrack [20] achieves an optimal accuracy-speed trade-off via dynamic layer pruning, and NGDINO [19] aligns visual tracking with natural language by explicitly modeling object counts. However, these methods remain within the traditional detection paradigm [17, 4, 6, 18, 5, 19, 20], neglecting the UAV’s intrinsic motion characteristics and the potential for embodied active tracking.

VAT, the predecessor to EVT, achieves continuous target locking through autonomous motion and perspective adjustments. Recent advancements in VAT encompass open-world benchmarks [8], 3D anti-distractor tracking [7], and end-to-end control [21, 9, 22]. Specifically, GC-VAT [8] utilizes goal-centered rewards and curriculum learning for dynamic environments, whereas Ad-AOT [7] introduces reinforcement learning to navigate 3D distractors. D-VAT [9] enables zero-fine-tuning simulation-to-real transfer for continuous micro-aerial vehicle control, and CEL [22] resolves training divergence caused by anomalies via a cognitive embodied learning approach. Nevertheless, these VAT methods lack the capacity for complex natural language understanding, hindering their application in advanced semantic tasks.

EVT integrates perception and action decision-making to achieve continuous tracking through an embodied loop [23, 24, 25, 26, 15, 27]. To overcome VAT’s semantic limitations, recent EVT research increasingly incorporates VLA models for instruction-driven tracking. For example, HIEVT [24] uses spatial targets to bridge language and actions, while a VLM-enhanced framework [25] introduces self-reflection to recover from tracking failures. Furthermore,

Table 1: Comparison of Existing UAV Tracking and Embodied AI Benchmarks

Benchmark	Emboied Tracking	Kinematic Diversity	Language	Continuous Motion	UAV Dedicated
DAT[8]	✓	✓	✗	✓	✓
AD-AOT[7]	✓	✗	✗	✗	✓
RefDrone[19]	✗	✓	✓	✗	✓
IndoorUAV[14]	✗	✗	✓	✓	✓
UAV-Flow/UAV-Flow-Sim[37]	✗	✗	✓	✓	✓
VLA-AN[16]	✓	✗	✓	✓	✓
EVT-Bench[15]	✓	✗	✓	✓	✗
UC-EVT[24]	✓	✗	✓	✓	✗
UAV-Track (Ours)	✓	✓	✓	✓	✓

TrackVLA [15] leverages a shared LLM backbone to synchronize target recognition with trajectory planning, while TrackVLA++ [26] introduces Polar Chain-of-Thought to enhance robustness against severe occlusions.

2.2 VLA Models in Aerial Robotics

The rapid progress in EVT is driven by VLA models’ cross-modal fusion and continuous action generation capabilities [28, 11, 12]. Following the foundational multimodal synergy established by RT-1 and RT-2 [10, 29], models like OpenVLA and π_0 utilized technologies such as action chunking, flow-matching, dual systems and diffusion architectures to achieve efficient continuous action generation under multimodal inputs [30, 11, 12, 31, 32, 33]. Recently, the integration of reinforcement learning (e.g., $\pi_{0.6}$, GR-RL) has further propelled VLA models toward high-precision real-world manipulation [28, 34, 35, 36].

Leveraging their semantic and action-mapping strengths, VLA models are increasingly applied to UAVs. While current applications primarily focus on spatial navigation and obstacle avoidance [14, 37, 38] using enhanced visual reasoning or hierarchical architectures [16, 38, 39], some studies have extended VLA to high-speed drone racing [40], real-time human recognition [41], and aerial manipulation [42]. However, existing end-to-end flight control methods mostly target static interactions and struggle with highly dynamic tracking. Although preliminary trajectory tracking exists [16], a substantial gap remains for urban scenarios, where vehicles and pedestrians exhibit severe motion randomness, frequent occlusions, and background interference. Developing an end-to-end VLA system capable of maintaining advanced semantic locking and ultra-low latency dynamic interaction in such volatile environments remains an urgent challenge that this paper seeks to address.

3 UAV-Track Benchmark

3.1 Problem Formulation

In this section, we introduce UAV-Track, a novel benchmark for natural language-guided Unmanned Aerial Vehicle visual tracking, which we formulate as an end-to-end sequential decision-making problem. By fusing the multimodal context \mathcal{O}_t , the VLA model directly outputs the relative pose of the target and the low-level action trajectory. At time step t , the system receives three types of input observations:

Language Instruction: $L = \{w_1, \dots, w_m\}$: Describes the target’s appearance and the specific flight intention. Visual Observations: $I_{t-3:t} \in \mathbb{R}^{4 \times H \times W \times 3}$: Comprises the current and three previous front-view RGB image frames (detailed parameters are provided in the supplementary material). For the initial stage where $t < 4$, we employ a zero-padding strategy using black frames to maintain structural consistency in the temporal dimension. Proprioceptive State: $S_t = [\mathbf{v}_t, \dot{\psi}_t]^\top \in \mathbb{R}^4$: Includes the 3D linear velocity (m/s) and the body yaw rate(rad/s). To reduce the complexity of policy learning, we fix the pitch and roll angles of the UAV as well as the camera extrinsics in the simulation.

Based on the above inputs, the model simultaneously performs spatial perception and flight control prediction:

Target Relative Pose Perception: Outputs the pose of the tracked target in the UAV-centric coordinate system, which is formulated as $P_t = [\Delta x_t^{\text{tar}}, \Delta y_t^{\text{tar}}, \Delta z_t^{\text{tar}}, \Delta \psi_t^{\text{tar}}]^\top \in \mathbb{R}^4$. This includes the 3D relative position and the horizontal yaw offset, providing precise geometric guidance. Future Action Trajectory: Adopts an action chunking strategy to predict a sequence of continuous commands for the future k steps ($k = 25$ in our implementation), defined as $A_{t+1:t+k} = \{\mathbf{a}_t + 1, \dots, \mathbf{a}_{t+k}\}$. The action vector $\mathbf{a}_i = [\Delta x_i^{\text{act}}, \Delta y_i^{\text{act}}, \Delta z_i^{\text{act}}, \Delta \psi_i^{\text{act}}]^\top \in \mathbb{R}^4$ directly represents the desired 3D relative displacement and yaw angle change, discarding traditional velocity control to perfectly align the action space with the perception output.

3.2 Simulation and Data Collection

To bridge the sim-to-real gap, we build a comprehensive data collection environment and processing pipeline based on CARLA that encompasses diverse topological scenes, dynamic weather, and varying lighting conditions. We adopt a hybrid strategy to collect large-scale trajectory data. First, human experts control the UAV to collect high-quality demonstrations, providing a baseline for spatial reasoning and fallback strategies for corner cases. Subsequently, we deploy an automated algorithm based on the Artificial Potential Field (APF) method for data augmentation[43]. During automatic cruising, we dynamically inject random perturbations into the control commands to force the UAV off its ideal trajectory, and the APF generates recovery paths. This mechanism effectively alleviates the covariate shift problem common in end-to-end imitation learning, teaching the model to recover autonomously and significantly enhancing closed-loop robustness.

3.3 Statistics

This benchmark collects a total of 892,756 frames of multimodal trajectory data, comprising approximately 200K frames of expert demonstrations and 690K frames of automated collection data, covering 85 diverse objects and 176 fine-grained tracking tasks. As shown in Figure 2, our dataset achieves comprehensive scenario coverage across three core dimensions:

Environment and Target Diversity: Covers dynamic weather, a full range of tracking distances, and three main categories of dynamic targets. **Kinematic Completeness:** Encompasses a wide range of target speeds (0 - 70 m/s) and UAV yaw dynamics, supporting the learning of physically feasible policies. **Language Instruction Generalization:** Hundreds of natural language instructions support cross-modal task evaluation.

Compared to existing benchmarks (Table 1), this work is the first dedicated embodied UAV tracking benchmark that comprehensively supports natural language guidance and 4-DoF continuous motion, demonstrating significant advantages in scene generalization and task universality.

3.4 Evaluation Metrics

We introduce two core metrics to measure the closed-loop tracking robustness of the system. Considering the complex occlusions in real-world scenarios, we allow the model to autonomously recover after briefly losing the target:

3.4.1 Success Rate (SR)

Given the total number of test episodes N , we define a binary indicator function $\mathbb{I}_{\text{success}}^{(i)}$. Episode i is considered successful ($\mathbb{I}_{\text{success}}^{(i)} = 1$) only if it does not trigger a "fatal failure" during its execution period T_i . A fatal failure is defined as: the target continuously deviates from the effective distance range ($d_t \notin [d_{\min}, d_{\max}]$ or completely leaves the field of view) for a duration exceeding the maximum tolerance threshold τ . The overall success rate is defined as $\text{SR} = \frac{1}{N} \sum_{i=1}^N \mathbb{I}_{\text{success}}^{(i)}$.

3.4.2 Average Tracked Frames (ATF)

ATF provides a more fine-grained process evaluation, measuring the average duration of maintaining effective tracking before a fatal failure occurs. For an episode with a maximum step limit of T_i , if a valid control is output and the target is within the effective range at a single step t , then $\mathbb{I}_{\text{track}}^{(i,t)} = 1$; once a fatal failure is triggered, all subsequent steps are set to zero. The metric is calculated as $\text{ATF} = \frac{1}{N} \sum_{i=1}^N \sum_{t=1}^{T_i} \mathbb{I}_{\text{track}}^{(i,t)}$. This metric intuitively reflects the differences in control stability among models when handling complex dynamics.

4 UAV-Track VLA

To address the limitations of general VLA models in continuous UAV tracking—specifically, their inadequate temporal modeling for historical frames and the severe mismatch between high-level semantic features and low-level continuous displacement control—we propose an improved UAV VLA tracking architecture tailored for complex urban scenarios. Built upon the open-source $\pi_{0.5}$ model, our approach introduces a temporal compression net and a spatial-aware auxiliary grounding head. By employing an end-to-end training strategy with a mixed loss function, our model effectively bridges the gap between high-level semantic understanding and high-frequency continuous control.

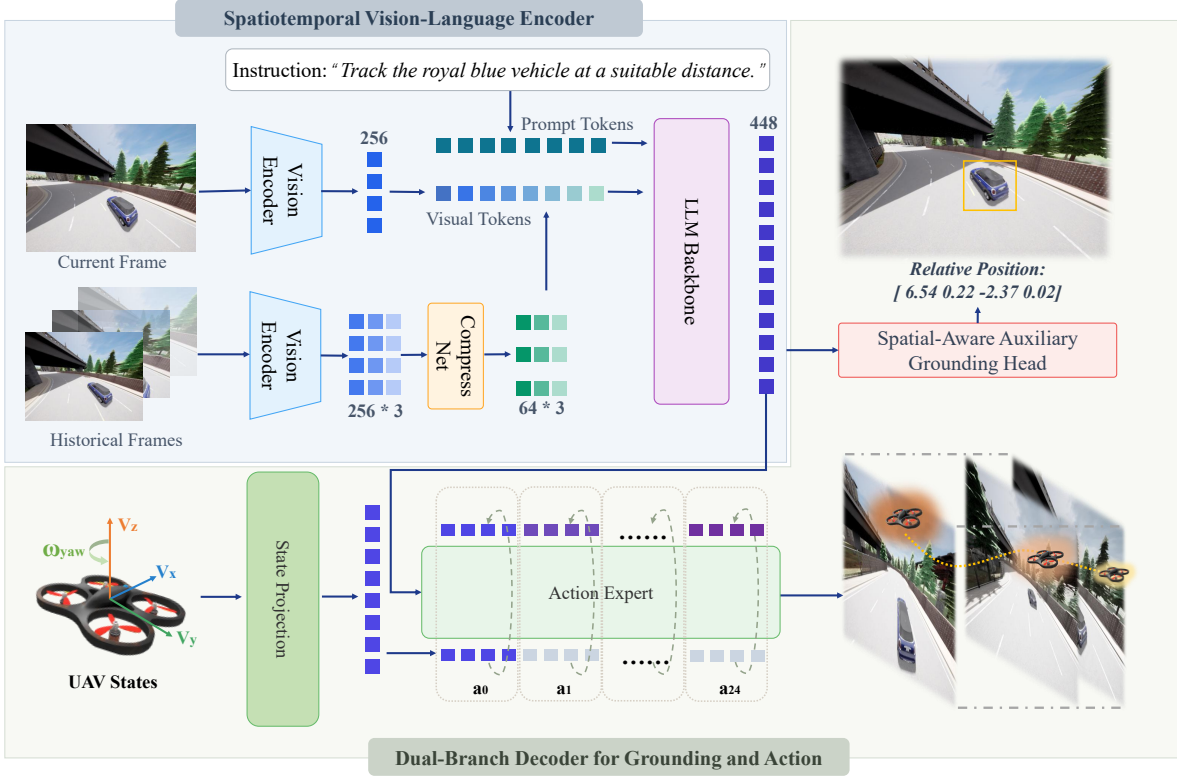


Figure 3: **Overall architecture of our proposed UAV-Track VLA model.** The model processes heterogeneous inputs through a spatiotemporal encoder and parallel decoders. Within the encoder, historical frames are temporally compressed and concatenated with the current frame to capture dynamic evolution, then fused with the instruction via an LLM. The shared multimodal features are subsequently dispatched to two decoupled branches: a spatial-aware auxiliary grounding head that predicts the target’s relative pose P_t to inject precise geometric priors for robust high-frequency control

Our model adopts an encoder-dual-branch decoder hierarchical architecture. This design aims to assist the encoder in achieving precise spatial alignment of multimodal features without compromising the continuous control capabilities of the action expert. As illustrated in Figure 3, the model takes heterogeneous inputs: a visual sequence containing current and historical observations $I_{t-3:t}$, a natural language instruction L , and the current proprioceptive state of the UAV S_t . After the encoder transforms these inputs into high-dimensional cross-modal features, two parallel decoding branches process them to output the target’s relative pose P_t for auxiliary supervision and a 25-step continuous action displacement sequence $A_{t+1:t+25}$ for high-frequency control.

4.1 Spatiotemporal vision-language encoder

The encoder integrates a visual feature extraction module, a temporal compression net, and a foundational large vision-language model (PaliGemma[44]) to transform the heterogeneous inputs into high-dimensional cross-modal features enriched with temporal context and language semantics.

4.1.1 Backbone

Our model utilizes PaliGemma as its core foundational architecture. Specifically, the vision tower (SigLIP[45]) extracts image features, mapping single-frame images into visual tokens within the semantic feature space. Concurrently, the language instruction is processed by a tokenizer to generate instruction tokens. Subsequently, the Large Language Model (Gemma[46]) performs deep fusion and cross-modal interaction between the mapped visual semantic features and the textual semantic features.

4.1.2 Temporal compression net

Capturing the dynamic motion trends of targets necessitates the incorporation of historical visual information. To prevent the exponential growth in computational dimensions and feature redundancy caused by stacking multiple frames, we introduce a lightweight Temporal compression net prior to feature injection into Gemma. Specifically, for the three historical frames $I_{t-3:t-1}$, this module employs a linear projection layer to drastically compress the 256 visual tokens of each single frame down to 64 tokens. These 64×3 low-dimensional tokens are then concatenated with the 256 original tokens of the current frame along the temporal dimension, resulting in a cohesive set of 448 visual features embedded with temporal information. To enhance the model’s ability to capture temporal dependencies across the input image sequence, we explicitly introduce a Learnable Positional Encoding, enabling the model to accurately extract the evolutionary patterns between frames. Ultimately, this comprehensive visual feature set is fed into Gemma alongside the instruction tokens for joint encoding.

4.2 Dual-Branch decoder for grounding and action

To prevent representational conflicts between explicit spatial grounding features and continuous action generation, we design a parallel dual-branch decoding structure comprising a spatial-aware auxiliary grounding head and a flow matching action expert. These two branches share the cross-modal features but remain completely decoupled during forward inference.

4.2.1 Spatial-aware auxiliary grounding head

To address the specific requirements of continuous tracking and the lack of precise spatial geometric priors when applying general VLA models to this task, we attach a compact transformer after Gemma to serve as the spatial-aware auxiliary grounding head. Taking cross-modal features as input, this module predicts the 3D relative position and horizontal yaw angle deviations of the target relative to the UAV. Crucially, this branch adopts a Bypass Auxiliary Design that operates exclusively via auxiliary supervision during the training phase. By backpropagating this spatial loss, the mechanism compels the encoder to embed accurate task-specific geometric priors into the cross-modal tokens, thereby establishing a robust feature foundation for subsequent continuous action planning.

4.2.2 Flow matching action expert

The action planning branch adopts a flow matching architecture, which effectively transforms discrete step predictions into flow field fitting within a continuous state space, highly aligning with the high-frequency continuous control demands of UAVs. This branch concatenates the cross-modal features—now imbued with spatial priors—with the UAV’s proprioceptive state S_t . By learning to approximate the displacement flow field of the ideal tracking trajectory, the model performs continuous inference, ultimately generating a 25-step continuous displacement control sequence $A_{t+1:t+25}$.

4.3 Objectives

To fulfill the cross-modal alignment requirements of vision, language, and action in complex urban scenarios, we design an end-to-end joint training strategy based on a mixed loss function. This strategy synchronizes the optimization of the encoder, the spatial-aware auxiliary grounding head, and the flow matching action expert, achieving simultaneous cross-modal representation alignment and rational action generation within a single training process.

The total loss function of our model is a weighted fusion of the position loss and the flow matching loss. The core objective of this design is to optimize the effective mapping from spatial features to continuous control actions within the action expert, while leveraging the position loss to ensure the encoder’s cross-modal features possess accurate geometric priors as a prerequisite.

The total loss function is defined as:

$$L_{total} = \lambda_1 L_{pos} + \lambda_2 L_{action}$$

where L_{pos} denotes the position loss, which supervises the 3D position and yaw angle deviation predictions of the spatial-aware auxiliary grounding head, implicitly constraining the encoder’s capacity to model spatial geometric information. L_{action} represents the flow matching loss, acting as the core of the network optimization to supervise the generation quality of the continuous displacement sequence by the flow matching action expert, ensuring the physical rationality and smoothness of the UAV’s 25-step action output. λ_1 and λ_2 are weight coefficients. By judiciously adjusting their ratio, the model prioritizes enhancing the generation quality of the action expert’s continuous control,

Table 2: Quantitative results on Seen Maps

Model	Target	Close		Suitable		Far	
		ATF	SR (%)	ATF	SR (%)	ATF	SR (%)
ACT[47]	Veh. / Ped.	36.00 / 18.50	0.00 / 0.00	30.17 / 20.70	0.00 / 0.00	33.24 / 21.52	0.00 / 0.00
WALL-OSS[48]	Veh. / Ped.	25.67 / 44.51	0.00 / 0.00	47.80 / 55.88	0.00 / 2.44	40.29 / 41.62	0.00 / 0.00
π_0 [12]	Veh. / Ped.	67.14 / 86.27	1.43 / 0.00	94.53 / 142.78	7.35 / 18.75	89.14 / 133.53	3.39 / 17.65
$\pi_{0.5}$ [34]	Veh. / Ped.	81.07 / 110.44	5.56 / 7.41	138.55 / 191.97	22.54 / 28.57	174.81 / 214.28	33.90 / 44.44
UAV-Track VLA (Ours)	Veh. / Ped.	98.47 / 203.93	12.73 / 31.82	164.79 / 263.61	29.61 / 60.20	194.91 / 269.65	37.88 / 61.76

Table 3: Zero-shot performance on Unseen Maps

Model	Target	Close		Suitable		Far	
		ATF	SR (%)	ATF	SR (%)	ATF	SR (%)
ACT[47]	Veh. / Ped.	31.21 / 18.35	0.00 / 0.00	31.61 / 18.65	0.00 / 0.00	39.14 / 19.71	0.00 / 0.00
WALL-OSS[48]	Veh. / Ped.	29.63 / 39.30	0.00 / 0.00	46.59 / 52.56	0.00 / 0.00	34.78 / 41.82	0.00 / 0.00
π_0 [12]	Veh. / Ped.	76.05 / 84.83	2.63 / 4.35	95.22 / 148.20	10.00 / 20.00	76.91 / 146.42	2.22 / 21.05
$\pi_{0.5}$ [34]	Veh. / Ped.	83.49 / 130.86	4.88 / 23.81	201.72 / 135.38	33.33 / 23.81	128.20 / 139.18	17.07 / 5.88
UAV-Track VLA (Ours)	Veh. / Ped.	75.56 / 148.94	6.67 / 29.41	150.00 / 210.24	29.79 / 36.84	159.84 / 226.90	27.91 / 55.00

while utilizing the spatial grounding supervision to provide a reliable feature foundation, ultimately achieving optimal overall performance in multimodal continuous tracking.

5 Experiments

5.1 Experimental Setup

To systematically evaluate the performance of the proposed UAV-Track VLA in complex dynamic environments, all experiments are conducted within the CARLA simulator. At the onset of each evaluation episode, the UAV is initialized at a random position behind and above the target to perform end-to-end embodied visual tracking. To ensure standardized evaluation, the maximum duration of each episode is set to 500 steps. To provide a comprehensive analysis, the experimental results are categorized and reported based on two primary target types: vehicles (including two-wheelers) and pedestrians. Detailed environmental parameters, including weather conditions and initialization offsets, are provided in the supplementary material.

EVT requires the UAV to maintain both semantic locking and physical following of the target in 3D space. A tracking state is considered valid only when the target’s bounding box remains within the camera’s Field of View (FOV). To assess the model’s fine-grained understanding of spatial prepositions in natural language instructions, we define three distance-based tracking criteria: close, suitable, and long. Specifically, for vehicles, the close, suitable, and long distances are defined as $\leq 25m$, $\leq 35m$, and $\leq 40m$, respectively. For pedestrians, owing to their smaller scale, these corresponding thresholds are inherently tighter, set at $\leq 10m$, $\leq 15m$, and $\leq 20m$.

The outcome of a tracking mission is determined by the following criteria: a mission is terminated and marked as a failure if an abnormal tracking state (i.e., violating FOV or distance constraints) persists for 15 consecutive frames. A task achieves success simply by surviving a 200-step episode without ever triggering this continuous failure condition.

UAV-Track VLA is optimized end-to-end using a joint loss function. As detailed in the methodology section, this joint objective aligns visual features with language instructions while supervising action execution. Specific weight configurations for each loss component are detailed in the supplementary material. The model is trained on two NVIDIA H100 GPUs with a global batch size of 64 for 45,000 iterations. We utilize absolute position changes as the primary supervision signal, enabling the flow-matching action expert to effectively fit the action flow field in a continuous state space.

5.2 Quantitative Results and Analysis

We compare UAV-Track VLA against several baselines, including π_0 , the original $\pi_{0.5}$, and traditional control-based methods. Average results across multiple towns are summarized in Tables 2 and 3.

In seen maps (Town02, Town05, Town06, Town07, Town10HD), UAV-Track VLA demonstrates superior adaptability across diverse target types and motion patterns. As shown in Table 2, our model achieves high success rates (SR) and

Table 4: Ablation Study: Impact of the Spatial Auxiliary Head

Map Type	Setting	Target	Close		Suitable		Far	
			ATF	SR (%)	ATF	SR (%)	ATF	SR (%)
Seen	w/o Aux Head	Veh. / Ped.	80.45 / 125.43	10.45 / 10.00	176.13 / 166.67	29.87 / 23.33	161.76 / 183.96	30.88 / 39.29
	UAV-Track VLA	Veh. / Ped.	98.47 / 203.93	12.73 / 31.82	164.79 / 263.61	29.61 / 60.20	194.91 / 269.65	37.88 / 61.76
Unseen	w/o Aux Head	Veh. / Ped.	70.22 / 96.96	3.12 / 12.50	174.24 / 137.48	26.83 / 8.70	120.98 / 159.22	16.67 / 22.22
	UAV-Track VLA	Veh. / Ped.	75.56 / 148.94	6.67 / 29.41	150.00 / 210.24	29.79 / 36.84	159.84 / 226.90	27.91 / 55.00

average tracking steps. For instance, in the "Far" pedestrian tracking task, UAV-Track VLA achieves an average of 269.65 steps with a 61.76% SR, significantly outperforming all baseline models. For the vehicle tracking task under the same distance constraint, the average steps reach 194.91 with a 37.88% SR.

To evaluate robustness, we deploy the model in entirely unseen CARLA towns (Town01, Town03, Town04). Results in Table 3 indicate that UAV-Track VLA maintains stable performance even without environment priors. For pedestrian tracking at "Suitable" and "Far" distances, the model retains an average of 210.24 and 226.90 steps, respectively, with SRs only slightly lower than those in seen maps. These results validate the model's effective performance and strong generalization ability in unseen scenes.

A key observation is that while UAV-Track VLA performs comparably to the original $\pi_{0.5}$ on vehicle tracking, it shows a substantial lead in pedestrian tracking. In unseen maps ("Far" distance), $\pi_{0.5}$'s SR for pedestrians drops to 5.88%, whereas UAV-Track VLA maintains 55.00%. This clearly demonstrates the significant advantage of our improved model when handling pedestrian targets compared to vehicle targets.

Table 5: Inference Efficiency Comparison

Model	Average Latency (s)
WALL-OSS[48]	0.4524
$\pi_{0.5}$ [34]	0.0857
π_0 [12]	0.0691
UAV-Track VLA (Ours)	0.0571

5.3 Ablation Analysis

5.3.1 Effectiveness of the Auxiliary Head.

We investigate the contribution of the spatial auxiliary head by comparing the full UAV-Track VLA against a variant without this module (denoted as *w/o Aux Head* in Table 4). The absence of the auxiliary head leads to a severe performance decay in pedestrian tracking tasks. In seen maps ("Far"), the average steps drop from 269.65 to 183.96, and the SR falls from 61.76% to 37.88%. This performance gap is even more pronounced in unseen maps, dropping from 226.90 steps to 159.22 steps. These results demonstrate that the auxiliary head is essential for achieving precise vision-language alignment and spatial distance estimation, which is critical for maintaining accurate distances during pedestrian tracking.

5.3.2 Inference Efficiency.

To evaluate the real-time control capabilities, we conduct a timing analysis of the single-step continuous inference latency across different models. To ensure a fair and meaningful evaluation, our comparison focuses strictly on models with similar parameter scales. Consequently, the ACT model is excluded from this analysis due to its significantly smaller parameter size and distinct architecture. Based on a statistical analysis of approximately 1,200 valid data points per model, the average inference latency is summarized in Table 5. The results reveal that while the original $\pi_{0.5}$ requires 0.0857s per step, our UAV-Track VLA reduces the average latency to 0.0571s, achieving a substantial 33.4% improvement in computational efficiency. This efficiency gain is primarily attributed to the temporal compression net, which effectively eliminates the redundancy of multi-frame inputs while preserving essential temporal context for high-precision tracking.

6 Conclusion

In this paper, we presented UAV-Track VLA, a novel end-to-end embodied visual tracking framework designed to tackle the highly dynamic and complex nature of urban UAV tracking. To bridge the gap between high-level language semantics and high-frequency low-level flight control, we introduced a parallel dual-branch decoding architecture that effectively decouples spatial grounding from continuous action generation. By incorporating a temporal compression net and a spatial-aware auxiliary grounding head, our model efficiently extracts dynamic evolution patterns and injects precise geometric priors into the flow matching action expert. Furthermore, we proposed UAV-Track, a large-scale multimodal benchmark dedicated to natural language-guided embodied UAV tracking, comprising over 890K frames of highly diverse simulated data. Extensive experiments in the CARLA simulator demonstrate that our approach significantly outperforms existing baselines in tracking robustness, cross-modal alignment, and zero-shot generalization. Notably, our framework excels in complex pedestrian tracking scenarios while achieving a 33.4% reduction in single-step inference latency. In future work, we plan to deploy our framework on physical UAV platforms to further investigate sim-to-real transfer and real-world embodied tracking capabilities.

References

- [1] Yonglin Tian, Fei Lin, Yiduo Li, Tengchao Zhang, Qiyao Zhang, Xuan Fu, Jun Huang, Xingyuan Dai, Yutong Wang, Chunwei Tian, et al. Uavs meet llms: Overviews and perspectives towards agentic low-altitude mobility. *Information Fusion*, 122:103158, 2025.
- [2] Nianyi Sun, Jin Zhao, Qing Shi, Chang Liu, and Peng Liu. Moving target tracking by unmanned aerial vehicle: A survey and taxonomy. *IEEE Transactions on Industrial Informatics*, 20(5):7056–7068, 2024.
- [3] Wahab Khawaja, Martins Ezuma, Vasili Semkin, Fatih Erden, Ozgur Ozdemir, and Ismail Guvenc. A survey on detection, classification, and tracking of uavs using radar and communications systems. *IEEE Communications Surveys & Tutorials*, 2025.
- [4] Yiming Li, Changhong Fu, Fangqiang Ding, Ziyuan Huang, and Geng Lu. Autotrack: Towards high-performance visual tracking for uav with automatic spatio-temporal regularization. In *Proceedings of the IEEE/CVF Conference on Computer Vision and Pattern Recognition (CVPR)*, June 2020.
- [5] Shuiwang Li, Yangxiang Yang, Dan Zeng, and Xucheng Wang. Adaptive and background-aware vision transformer for real-time uav tracking. In *Proceedings of the IEEE/CVF international conference on computer vision*, pages 13989–14000, 2023.
- [6] Yuanliang Xue, Tao Shen, Guodong Jin, Lining Tan, Nian Wang, Lianfeng Wang, and Jing Gao. Handling occlusion in uav visual tracking with query-guided redetection. *IEEE Transactions on Instrumentation and Measurement*, 73:1–17, 2024.
- [7] Mao Xi, Yun Zhou, Zheng Chen, Wengang Zhou, and Houqiang Li. Anti-distractor active object tracking in 3d environments. *IEEE Transactions on Circuits and Systems for Video Technology*, 32(6):3697–3707, 2022.
- [8] Haowei Sun, Jinwu Hu, Zhirui Zhang, Haoyuan Tian, Xinze Xie, Yufeng Wang, Xiaohua Xie, Yun Lin, Zhuliang Yu, and Mingkui Tan. Open-world drone active tracking with goal-centered rewards. In *The Thirty-ninth Annual Conference on Neural Information Processing Systems*, 2025.
- [9] Alberto Dionigi, Simone Felicioni, Mirko Leomanni, and Gabriele Costante. D-vat: End-to-end visual active tracking for micro aerial vehicles. *IEEE Robotics and Automation Letters*, 9(6):5046–5053, 2024.
- [10] Anthony Brohan, Noah Brown, Justice Carbajal, Yevgen Chebotar, Joseph Dabis, Chelsea Finn, Keerthana Gopalakrishnan, Karol Hausman, Alex Herzog, Jasmine Hsu, Julian Ibarz, Brian Ichter, Alex Irpan, Tomas Jackson, Sally Jesmonth, Nikhil J Joshi, Ryan Julian, Dmitry Kalashnikov, Yuheng Kuang, Isabel Leal, Kuang-Huei Lee, Sergey Levine, Yao Lu, Utsav Malla, Deeksha Manjunath, Igor Mordatch, Ofir Nachum, Carolina Parada, Jodilyn Peralta, Emily Perez, Karl Pertsch, Jornell Quiambao, Kanishka Rao, Michael Ryoo, Grecia Salazar, Pannag Sanketi, Kevin Sayed, Jaspier Singh, Sumedh Sontakke, Austin Stone, Clayton Tan, Huang Tran, Vincent Vanhoucke, Steve Vega, Quan Vuong, Fei Xia, Ted Xiao, Peng Xu, Sichun Xu, Tianhe Yu, and Brianna Zitkovich. Rt-1: Robotics transformer for real-world control at scale, 2023.
- [11] Moo Jin Kim, Karl Pertsch, Siddharth Karamcheti, Ted Xiao, Ashwin Balakrishna, Suraj Nair, Rafael Rafailov, Ethan Foster, Grace Lam, Pannag Sanketi, Quan Vuong, Thomas Kollar, Benjamin Burchfiel, Russ Tedrake, Dorsa Sadigh, Sergey Levine, Percy Liang, and Chelsea Finn. Openvla: An open-source vision-language-action model, 2024.
- [12] Kevin Black, Noah Brown, Danny Driess, Adnan Esmail, Michael Equi, Chelsea Finn, Niccolo Fusai, Lachy Groom, Karol Hausman, Brian Ichter, Szymon Jakubczak, Tim Jones, Liyiming Ke, Sergey Levine, Adrian

- Li-Bell, Mohith Mothukuri, Suraj Nair, Karl Pertsch, Lucy Xiaoyang Shi, James Tanner, Quan Vuong, Anna Walling, Haohuan Wang, and Ury Zhilinsky. π_0 : A vision-language-action flow model for general robot control, 2026.
- [13] Sicong Jiang, Zilin Huang, Kangan Qian, Ziang Luo, Tianze Zhu, Yang Zhong, Yihong Tang, Menglin Kong, Yunlong Wang, Siwen Jiao, et al. A survey on vision-language-action models for autonomous driving. In *Proceedings of the IEEE/CVF International Conference on Computer Vision*, pages 4524–4536, 2025.
- [14] Xu Liu, Yu Liu, Hanshuo Qiu, Yang Qirong, and Zhouhui Lian. Indooruav: Benchmarking vision-language uav navigation in continuous indoor environments, 2025.
- [15] Shaoan Wang, Jiazhao Zhang, Minghan Li, Jiahang Liu, Anqi Li, Kui Wu, Fangwei Zhong, Junzhi Yu, Zhizheng Zhang, and He Wang. Trackvla: Embodied visual tracking in the wild. In Joseph Lim, Shuran Song, and Hae-Won Park, editors, *Proceedings of The 9th Conference on Robot Learning*, volume 305 of *Proceedings of Machine Learning Research*, pages 4139–4164. PMLR, 27–30 Sep 2025.
- [16] Yuze Wu, Mo Zhu, Xingxing Li, Yuheng Du, Yuxin Fan, Wenjun Li, Zhichao Han, Xin Zhou, and Fei Gao. Vla-an: An efficient and onboard vision-language-action framework for aerial navigation in complex environments, 2025.
- [17] Dengdi Sun, Leilei Cheng, Song Chen, Chenglong Li, Yun Xiao, and Bin Luo. Uav-ground visual tracking: A unified dataset and collaborative learning approach. *IEEE Transactions on Circuits and Systems for Video Technology*, 34(5):3619–3632, 2023.
- [18] You Wu, Yongxin Li, Mengyuan Liu, Xucheng Wang, Xiangyang Yang, Hengzhou Ye, Dan Zeng, Qijun Zhao, and Shuiwang Li. Learning an adaptive and view-invariant vision transformer for real-time uav tracking. *IEEE Transactions on Circuits and Systems for Video Technology*, 2025.
- [19] Zhichao Sun, Yepeng Liu, Zhiling Su, Huachao Zhu, Yuliang Gu, Yuda Zou, Zelong Liu, Gui-Song Xia, Bo Du, and Yongchao Xu. Refdrone: A challenging benchmark for referring expression comprehension in drone scenes. *arXiv preprint arXiv:2502.00392*, 2025.
- [20] Chaocan Xue, Bineng Zhong, Qihua Liang, Yaozong Zheng, Ning Li, Yuanliang Xue, and Shuxiang Song. Similarity-guided layer-adaptive vision transformer for uav tracking. In *Proceedings of the IEEE/CVF Conference on Computer Vision and Pattern Recognition (CVPR)*, pages 6730–6740, June 2025.
- [21] Wenhan Luo, Peng Sun, Fangwei Zhong, Wei Liu, Tong Zhang, and Yizhou Wang. End-to-end active object tracking and its real-world deployment via reinforcement learning. *IEEE Transactions on Pattern Analysis and Machine Intelligence*, 42(6):1317–1332, 2020.
- [22] Qihui Wu, Jiahao Li, Fuhui Zhou, Jiahuan Ji, Haoyang Wang, Hongtao Liang, and Kai-Kuang Ma. Cognitive embodied learning for anomaly active target tracking. *Communications Engineering*, 4(1):224, Nov 2025.
- [23] Jiazhao Zhang, Kunyu Wang, Shaoan Wang, Minghan Li, Haoran Liu, Songlin Wei, Zhongyuan Wang, Zhizheng Zhang, and He Wang. Uni-navid: A video-based vision-language-action model for unifying embodied navigation tasks, 2025.
- [24] Kui Wu, Hao Chen, Churan Wang, Fakhri Karray, Zhoujun Li, Yizhou Wang, and Fangwei Zhong. Hierarchical instruction-aware embodied visual tracking, 2025.
- [25] Kui Wu, Shuhang Xu, Hao Chen, Churan Wang, Zhoujun Li, Yizhou Wang, and Fangwei Zhong. Vlm can be a good assistant: Enhancing embodied visual tracking with self-improving vision-language models. In *2025 IEEE/RSJ International Conference on Intelligent Robots and Systems (IROS)*, pages 13154–13161, 2025.
- [26] Jiahang Liu, Yunpeng Qi, Jiazhao Zhang, Minghan Li, Shaoan Wang, Kui Wu, Hanjing Ye, Hong Zhang, Zhibo Chen, Fangwei Zhong, Zhizheng Zhang, and He Wang. Trackvla++: Unleashing reasoning and memory capabilities in vla models for embodied visual tracking, 2025.
- [27] Fangwei Zhong, Kui Wu, Churan Wang, Hao Chen, Hai Ci, Zhoujun Li, and Yizhou Wang. Unrealzoo: Enriching photo-realistic virtual worlds for embodied ai. In *Proceedings of the IEEE/CVF International Conference on Computer Vision (ICCV)*, pages 5769–5779, October 2025.
- [28] Chilam Cheang, Sijin Chen, Zhongren Cui, Yingdong Hu, Liquan Huang, Tao Kong, Hang Li, Yifeng Li, Yuxiao Liu, Xiao Ma, Hao Niu, Wenxuan Ou, Wanli Peng, Zeyu Ren, Haixin Shi, Jiawen Tian, Hongtao Wu, Xin Xiao, Yuyang Xiao, Jiafeng Xu, and Yichu Yang. Gr-3 technical report, 2025.
- [29] Anthony Brohan, Noah Brown, Justice Carbajal, Yevgen Chebotar, Xi Chen, Krzysztof Choromanski, Tianli Ding, Danny Driess, Avinava Dubey, Chelsea Finn, Pete Florence, Chuyuan Fu, Montse Gonzalez Arenas, Keerthana Gopalakrishnan, Kehang Han, Karol Hausman, Alexander Herzog, Jasmine Hsu, Brian Ichter, Alex Irpan, Nikhil Joshi, Ryan Julian, Dmitry Kalashnikov, Yuheng Kuang, Isabel Leal, Lisa Lee, Tsang-Wei Edward Lee, Sergey Levine, Yao Lu, Henryk Michalewski, Igor Mordatch, Karl Pertsch, Kanishka Rao, Krista Reymann, Michael

- Ryoo, Grecia Salazar, Pannag Sanketi, Pierre Sermanet, Jaspiar Singh, Anikait Singh, Radu Soricut, Huong Tran, Vincent Vanhoucke, Quan Vuong, Ayzaan Wahid, Stefan Welker, Paul Wohlhart, Jialin Wu, Fei Xia, Ted Xiao, Peng Xu, Sichun Xu, Tianhe Yu, and Brianna Zitkovich. Rt-2: Vision-language-action models transfer web knowledge to robotic control, 2023.
- [30] Octo Model Team, Dibya Ghosh, Homer Walke, Karl Pertsch, Kevin Black, Oier Mees, Sudeep Dasari, Joey Hejna, Tobias Kreiman, Charles Xu, Jianlan Luo, You Liang Tan, Lawrence Yunliang Chen, Pannag Sanketi, Quan Vuong, Ted Xiao, Dorsa Sadigh, Chelsea Finn, and Sergey Levine. Octo: An open-source generalist robot policy, 2024.
- [31] Haoming Song, Delin Qu, Yuanqi Yao, Qizhi Chen, Qi Lv, Yiwen Tang, Modi Shi, Guanghui Ren, Maoqing Yao, Bin Zhao, et al. Hume: Introducing system-2 thinking in visual-language-action model. *arXiv preprint arXiv:2505.21432*, 2025.
- [32] ByungOk Han, Jaehong Kim, and Jinhyeok Jang. A dual process vla: Efficient robotic manipulation leveraging vlm, 2024.
- [33] Qixiu Li, Yaobo Liang, Zeyu Wang, Lin Luo, Xi Chen, Mozheng Liao, Fangyun Wei, Yu Deng, Sicheng Xu, Yizhong Zhang, Xiaofan Wang, Bei Liu, Jianlong Fu, Jianmin Bao, Dong Chen, Yuanchun Shi, Jiaolong Yang, and Baining Guo. Cogact: A foundational vision-language-action model for synergizing cognition and action in robotic manipulation, 2024.
- [34] Physical Intelligence, Kevin Black, Noah Brown, James Darpinian, Karan Dhabalia, Danny Driess, Adnan Esmail, Michael Equi, Chelsea Finn, Niccolo Fusai, Manuel Y. Galliker, Dibya Ghosh, Lachy Groom, Karol Hausman, Brian Ichter, Szymon Jakubczak, Tim Jones, Liyiming Ke, Devin LeBlanc, Sergey Levine, Adrian Li-Bell, Mohith Mothukuri, Suraj Nair, Karl Pertsch, Allen Z. Ren, Lucy Xiaoyang Shi, Laura Smith, Jost Tobias Springenberg, Kyle Stachowicz, James Tanner, Quan Vuong, Homer Walke, Anna Walling, Haohuan Wang, Lili Yu, and Ury Zhilinsky. $\pi_{0.5}$: a vision-language-action model with open-world generalization, 2025.
- [35] Physical Intelligence, Ali Amin, Raichelle Aniceto, Ashwin Balakrishna, Kevin Black, Ken Conley, Grace Connors, James Darpinian, Karan Dhabalia, Jared DiCarlo, Danny Driess, Michael Equi, Adnan Esmail, Yunhao Fang, Chelsea Finn, Catherine Glossop, Thomas Godden, Ivan Goryachev, Lachy Groom, Hunter Hancock, Karol Hausman, Gashon Hussein, Brian Ichter, Szymon Jakubczak, Rowan Jen, Tim Jones, Ben Katz, Liyiming Ke, Chandra Kuchi, Marinda Lamb, Devin LeBlanc, Sergey Levine, Adrian Li-Bell, Yao Lu, Vishnu Mano, Mohith Mothukuri, Suraj Nair, Karl Pertsch, Allen Z. Ren, Charvi Sharma, Lucy Xiaoyang Shi, Laura Smith, Jost Tobias Springenberg, Kyle Stachowicz, Will Stoeckle, Alex Swerdlow, James Tanner, Marcel Torne, Quan Vuong, Anna Walling, Haohuan Wang, Blake Williams, Sukwon Yoo, Lili Yu, Ury Zhilinsky, and Zhiyuan Zhou. $\pi_{0.6}^*$: a vla that learns from experience, 2025.
- [36] Yunfei Li, Xiao Ma, Jiafeng Xu, Yu Cui, Zhongren Cui, Zhigang Han, Liqun Huang, Tao Kong, Yuxiao Liu, Hao Niu, Wanli Peng, Jingchao Qiao, Zeyu Ren, Haixin Shi, Zhi Su, Jiawen Tian, Yuyang Xiao, Shenyu Zhang, Liwei Zheng, Hang Li, and Yonghui Wu. Gr-rl: Going dexterous and precise for long-horizon robotic manipulation, 2025.
- [37] Xiangyu Wang, Donglin Yang, Yue Liao, Wenhao Zheng, wenjun wu, Bin Dai, Hongsheng Li, and Si Liu. Uav-flow colosseo: A real-world benchmark for flying-on-a-word uav imitation learning, 2025.
- [38] Xiaolou Sun, Wufei Si, Wenhui Ni, Yuntian Li, Dongming Wu, Fei Xie, Runwei Guan, He-Yang Xu, Henghui Ding, Yuan Wu, Yutao Yue, Yongming Huang, and Hui Xiong. Autofly: Vision-language-action model for uav autonomous navigation in the wild, 2026.
- [39] Xijie Huang, Weiqi Gai, Tianyue Wu, Congyu Wang, Zhiyang Liu, Xin Zhou, Yuze Wu, and Fei Gao. Navdreamer: Video models as zero-shot 3d navigators, 2026.
- [40] Valerii Serpiva, Artem Lykov, Artyom Myshlyayev, Muhammad Haris Khan, Ali Alridha Abdulkarim, Oleg Sautenkov, and Dzmitry Tsetserukou. Racevla: Vla-based racing drone navigation with human-like behaviour, 2025.
- [41] Artem Lykov, Valerii Serpiva, Muhammad Haris Khan, Oleg Sautenkov, Artyom Myshlyayev, Grik Tadevosyan, Yasheerah Yaqoot, and Dzmitry Tsetserukou. Cognitivedrone: A vla model and evaluation benchmark for real-time cognitive task solving and reasoning in uavs, 2025.
- [42] Jianli Sun, Bin Tian, Qiyao Zhang, Chengxiang Li, Zihan Song, Zhiyong Cui, Yisheng Lv, and Yonglin Tian. Air-vla: Vision-language-action systems for aerial manipulation, 2026.
- [43] Herath Mpc Jayaweera and Samer Hanoun. A dynamic artificial potential field (d-apf) uav path planning technique for following ground moving targets. *IEEE access*, 8:192760–192776, 2020.

- [44] Lucas Beyer, Andreas Steiner, André Susano Pinto, Alexander Kolesnikov, Xiao Wang, Daniel Salz, Maxim Neumann, Ibrahim Alabdulmohsin, Michael Tschannen, Emanuele Bugliarello, et al. Paligemma: A versatile 3b vlm for transfer. *arXiv preprint arXiv:2407.07726*, 2024.
- [45] Xiaohua Zhai, Basil Mustafa, Alexander Kolesnikov, and Lucas Beyer. Sigmoid loss for language image pre-training. In *Proceedings of the IEEE/CVF international conference on computer vision*, pages 11975–11986, 2023.
- [46] Gemma Team, Thomas Mesnard, Cassidy Hardin, Robert Dadashi, Surya Bhupatiraju, Shreya Pathak, Laurent Sifre, Morgane Rivière, Mihir Sanjay Kale, Juliette Love, et al. Gemma: Open models based on gemini research and technology. *arXiv preprint arXiv:2403.08295*, 2024.
- [47] Tony Z. Zhao, Vikash Kumar, Sergey Levine, and Chelsea Finn. Learning fine-grained bimanual manipulation with low-cost hardware, 2023.
- [48] Andy Zhai, Brae Liu, Bruno Fang, Chalse Cai, Ellie Ma, Ethan Yin, Hao Wang, Hugo Zhou, James Wang, Lights Shi, Lucy Liang, Make Wang, Qian Wang, Roy Gan, Ryan Yu, Shalfun Li, Starrick Liu, Syllas Chen, Vincent Chen, and Zach Xu. Igniting vlms toward the embodied space, 2025.